Development 110, 311–323 (1990)
Printed in Great Britain © The Company of Biologists Limited 1990

daughterless-abo-like, a *Drosophila* maternal-effect mutation that exhibits abnormal centrosome separation during the late blastoderm divisions

WILLIAM SULLIVAN, JONATHAN S. MINDEN and BRUCE M. ALBERTS

Department of Biochemistry and Biophysics, University of California, San Francisco, San Francisco, California 94143-0448, USA

Summary

***daughterless-abo-like* (*dal*) is a maternal-effect semi-lethal mutation in *Drosophila*. The nuclear divisions of embryos derived from homozygous *dal* females are normal through nuclear cycle 10. However, during nuclear cycles 11, 12 and 13, a total of about half of the nuclei in each embryo either fail to divide or fuse with a neighboring nucleus during telophase. These abnormal nuclei eventually sink into the interior of the embryo, leaving their centrosomes behind on the surface. The loss of about one-half of the peripheral nuclei into the interior of the embryo results in these embryos cellularizing during nuclear cycle 14 with about one-half the normal number of cells. Surprisingly, many of these embryos develop a nearly normal larval cuticle and 8 % develop to adulthood.**

Observations of live embryos doubly injected with tubulin and histones that have been fluorescently labeled allows nuclear and centrosomal behavior to be directly followed as the embryo develops. We find that the abnormal nuclei arise from nuclei whose centrosomes have failed to separate normally in the previous interphase. These incompletely separated centrosomes can cause a non-functional spindle to form, leading to a nuclear division failure. Alternatively, they can form an abnormal spindle with a centrosome from a neighboring nucleus, causing two nuclei to share a common spindle pole. Such nuclei with a shared centrosome will undergo telophase fusions, unequal divisions, or division failures later in mitosis. These findings have helped us to understand the function of the centrosome in the *Drosophila* embryo.

Key words: *Drosophila*, embryo, centrosome, *daughterless-abo-like*, maternal-effect mutation, blastoderm.

Introduction

Many decades of observation have produced detailed descriptions of the morphological changes in mitosis. More recently, the analysis of the cell cycle has been extended to a molecular and biochemical level (Pickett-Heaps *et al.* 1982; McIntosh, 1984; Murray, 1989). One approach, pioneered by Hartwell and his colleagues in the yeast *Saccharomyces cerevisiae*, has identified genes coding for both structural and regulatory proteins that function in cell division (Hartwell *et al.* 1974; Hartwell, 1978). Isolating and characterizing cell cycle mutants is more difficult in *Drosophila* than in yeast. Most of the available *Drosophila* cell cycle mutants are non-conditional lethals (Smith *et al.* 1985; Gatti and Baker, 1989). In addition, the analysis often involves populations of cells with heterogeneous cell division programs and different developmental fates. In the early embryo, one is faced with the complication that a maternal contribution from the heterozygous mother is present in the homozygous mutant zygotes. Thus an embryo homozygous for a defective cell division gene may exhibit normal cell divisions due to the persistence of the maternally contributed wild-type gene product. But this is not the case for all genes affecting the cell cycle as shown by the zygotic phenotypes of the *string* and *cyclin A* cell cycle mutations (Edgar and O'Farrell, 1989; Lehner and O'Farrell, 1989).

After the initial embryonic divisions, the growth of the *Drosophila* larva is generally due to an increase in cell size rather than to cell division. In contrast, the imaginal discs grow by extensive cell division. Gatti and Baker reasoned that the initial nuclear and cellular divisions giving rise to the larval tissues should be primarily controlled by maternally supplied products, while imaginal disc cell proliferation that produces adult structures should be primarily zygotically controlled. As predicted, many larval-lethal discless mutations are disrupted in some aspect of cell division (Gatti and Baker, 1989).

A less-developed approach for finding cell division mutants in *Drosophila* involves searching for cell cycle mutations that affect the early embryo. The phenotype of such mutations can in principle be more readily studied, since the early nuclear cycles are short, nearly synchronous and well described both in terms of the division pattern and the cytoplasmic environment (Foe and Alberts, 1983; Zalokar and Erk, 1976). Most of the products influencing the early *Drosophila* embryo are supplied maternally, and mutations in the genes that

encode such products should have a maternal-effect. Thus, Zalokar and his colleagues characterized several maternal-effect mutations that are disrupted in the early syncytial divisions (Zalokar *et al.* 1975). In another maternal-effect mutation, *gnu,* rounds of DNA replication occur without accompanying nuclear divisions, and the centrosomes continue replicating independent of the nuclei, migrating to the periphery and initiating astral microtubule formation (Freeman *et al.* 1986; Freeman and Glover, 1987). More recently, Schupbach and Wieschaus (1989) have reported the results of an extensive screen for female sterile mutations on the second chromosome of *Drosophila.* They identified 67 complementation groups that display maternal-effect mutant phenotypes in which the homozygous mutant females lay morphologically normal eggs that do not develop normally. Some of these mutants are likely to be disrupted specifically in the syncytial nuclear divisions.

Here we describe the recessive maternal-effect mutation *daughterless-abo-like*, *dal*, as a gene that influences nuclear division in the early embryo only after the nuclei reach the cortical cytoplasm. Only a single allele of *dal* is available. Isolated by Sandler in a screen for mutations with reduced zygotic viability over the deficiency J-der-39 (31A,B–32E,F), *dal* is a member of a set of five maternal-effect genes that map to cytological region 31–32 and share an unusual property: the survival of embryos derived from homozygous females is increased according to the amount of paternally derived X and Y heterochromatin that each embryo receives (Sandler, 1977). The *dal*-derived embryos cellularize at about one-half of the wild-type density of surface nuclei and have an unusually large number of internal nuclei at this time (Sullivan, 1987). By studying fixed embryos, as well as living embryos that have been injected with fluorescently labeled histones and fluorescently labeled tubulin, we have characterized the initial defects and subsequent consequences that lead to the *dal* phenotype.

Materials and methods

Stocks

The isolation and the initial genetic characterization of *daughterless-abo-like (dal)* has been described (Sandler, 1977). Only a single allele was isolated and it is this allele that is used in this analysis. Unfortunately the only deficiency for the *dal* region (J-der-39) also includes M(2)fs, resulting in a dominant female sterility. This precluded us from examining eggs derived from mothers carrying the *dal* phenotype over a deficiency. In this paper, the experimental embryos were obtained from homozygous *dal* females crossed to wild-type Oregon-R males, and the control embryos were obtained from either heterozygous *dal* females or wild-type Oregon-R females crossed to wild-type Oregon-R males.

Egg to adult survival

Adult survival values were determined by egg-to-adult counts. Five hour egg collections were obtained from mass matings of flies of the desired genotype. The eggs were counted and transferred onto fresh media in half pint bottles. All of the flies eclosing prior to the 17th day after egg collection were scored as surviving adults.

Buffers

Embryos were fixed in PEM buffer which contains 0.1 M Pipes, 1 mM $MgCl_2$ and 1 mM Na_3EGTA adjusted to pH 6. 9 with KOH. The phosphate-buffered saline (PBS) is 0.01 M sodium phosphate, 0.15 M NaCl, adjusted to pH 7.3.

Fixation and immunofluorescence

For observing the nuclei in fixed embryos, we have used a modification of the procedure described by Mitchison and Sedat (1983). Embryos were dechorionated *en masse* in a 50 % bleach solution and extensively washed in 0.4 % NaCl and 0.03 % Triton X-100 (Karr and Alberts, 1986). These embryos were placed in a mixture of 10 parts heptane: 10 parts PEM buffer: 2 parts 37 % formaldehyde (J. T. Baker Chemical Company). After 12 min of vigorous shaking at room temperature, the lower aqueous layer was removed and an equal volume of 95 % methanol/5 % 0.5 M Na_3EGTA was added and shaken for 2 min. The devitellinized embryos sink, and after a wash in the methanol/EGTA solution, these embryos were transferred into a PBS solution. A 4 min transfer into PBS containing 1 $\mu g\,ml^{-1}$ 4–6-diamidino 2-phenylindole (DAPI) followed by extensive rinsing in PBS specifically stained the nuclei. For viewing, the embryos were mounted in a 50 % glycerol, 1 $mg\,ml^{-1}$ *N-N'*-1–4-phenylenediamine solution on a coverslip.

The nuclear cycle was determined during cycles 10–14 by counting the number of surface nuclei per a standard unit area, using a 5 mm×5 mm ocular grid (Foe and Alberts, 1983).

Determination of the relative amount of internal nuclear material

To determine the relative amount of internal nuclei during syncytial blastoderm, the nuclei of staged embryos were stained according to the procedure described above. Since these internal nuclei are dispersed throughout the interior of the embryo, a series of optical sections was used to obtain their number and distribution. In the studies presented below, we photographed the medial plane and sections 60 μm above and below this plane. In *dal*-derived embryos, the overabundance of nuclear staining material in the center of the embryo led to large clusters of staining material, making the task of counting individual nuclei difficult. Instead, we obtained a value that reflected the area taken up by the yolk nuclei relative to the area of the medial section of the embryo. Using an enlarger, tracings of the yolk nuclear distribution from three optical sections were transposed onto a sheet of paper and the ratio of the area taken up by the internal nuclei realtive to the area of the medial section of the embryo was determined. This procedure compresses a three-dimensional section into two dimensions. Area measurements were then made from resulting the two-dimensional surface.

Immunofluorescent staining of centrosomes in whole fixed Drosophila *embryos*

To observe the centrosomal staining pattern, we used a mammalian anti-neurofilament antibody (Amersham anti-200 kD neurofilament polypeptide, RPN1103). Surprisingly, this antibody reacts strongly with *Drosophila* centrosomes in embryos fixed by the following heat treatment (W. S. and C. Field, unpublished observation). About 0.3 ml of packed embryos is added to 10 ml of a 100 °C solution of 0.4 % NaCl, 0.03 % Triton X-100 and vortexed for 5 s. The eggs are

allowed to sink, the supernatant removed and ice cold 0.4 % NaCl, 0.03 % Triton X-100 solution is added. All subsequent operations are performed at room temperature. The embryos are allowed to sink and then treated with a 1:1 mixture of heptane: methanol/EGTA by shaking for 1 min. After soaking overnight in methanol/EGTA, the embryos are rehydrated through the series: 20 % PBS/80 % methanol, 40 % PBS/60 % methanol, 60 % PBS/40 % methanol, 80 % PBS/20 % methanol, and finally 100 % PBS (1 min each). Embryos fixed in this way stain normally for actin filaments (Miller *et al.* 1989), as well showing clear microtubule arrays (Douglas Kellogg, unpublished).

Embryos fixed with heat as described above were placed in a 1 % bovine serum albumin, 0.05 % Triton-X100 solution in PBS for 30 min (unless noted this is the solution used for all antibody dilutions and rinses). The embryos were then incubated for 1 h in a 1:100 dilution of the above antibody. After extensive rinsing, the embryos were stained for 1 h with a goat anti-mouse IgG coupled to rhodamine, followed by a 1 h rinse. Finally, the embryos were transferred into PBS that contained 1 $\mu g\,ml^{-1}$ DAPI for 4 min and then rinsed for 1 h in PBS.

Microscopy

For observing fixed embryos, we used both a Zeiss standard microscope equipped with epifluorescence and a Nikon Microphot-FXA with standard rhodamine and DAPI filter cassettes. The lenses included a Zeiss Pan-Neofluor 25/0.81 mm Ph2, Leitz Wetzlar PL APO 63/1.4 Oel, and a Nikon PlanApo 100 DM/Ph4.

In vivo *fluorescence analysis*

The *in vivo* analysis of nuclear behavior in *dal*-derived embryos was accomplished through a procedure developed by J.M. in which fluorescently labeled histones are microinjected into embryos and time-lapse images then taken using a fluorescence microscope (Minden *et al.* 1989). The *dal*-derived pre-cycle 10 embryos were prepared for microinjection by hand-dechorionation and mounting on a coverslip with a thin film of glue (prepared by dissolving double-stick tape in heptane). The histones, labeled with 5-(and 6)-carboxytetramethylrhodamine, succinimidyl ester(NHSR), were microinjected into these embryos and observed on an Olympus inverted microscope equipped for epifluorescence, using a 40/1.3 oil immersion objective lens (Olympus) and a rhodamine filter set (Omega Optical). The images were recorded with a CCD camera (Photometrics). Shutter control, lens focusing, fluorescent filter selection, data storage and data processing were regulated with a Microvax II workstation (Digital Equipment Corporation). The equipment and procedures are more fully described by Minden *et al.* (1989) and Agard *et al.* (1988). The data were stored on optical disc, and tracings on plastic sheets were made to follow the fate of selected nuclei through successive nuclear cycles. Spindle and centrosomal dynamics were examined in the same way using NHSR-labeled or 5-(and 6)-carboxyfluorescein, succinamidyl ester labeled (NHSF) microtubules injected into *Drosophila* embryos (Kellogg *et al.* 1988).

Results

The dal*-derived embryos cellularize at one-half of the normal nuclear density and have many more internal nuclei than normal embryos*

Embryos derived from homozygous *dal* females were fixed at cellular blastoderm and their nuclei stained with DAPI using a modification of the whole-mount method described by Karr and Alberts (1986). 76 % (76/100) of these embryos cellularized at a nuclear density approximately one-half the value found for normal embryos and had an excess of nuclei in the interior of the embryo (Fig. 1). An additional 14 % of the embryos exhibited distinct patches of peripheral nuclei during cellularization, some with average spacings greater than those typical of wild-type cycle 14 and others with average spacings less than the wild-type – in addition to an excess of internal nuclei (Sullivan, 1987). The remaining 10 % showed no development (a fraction of these are likely to be unfertilized). We do not understand the origin of either of these latter classes, and in this report we consider only the first and largest class.

The nuclei and cells in cellularized *dal*-derived embryos are much larger than the nuclei and cells in wild-type cycle 14 embryos, presumably because cellularization occurs at a reduced nuclear density equivalent to nuclear cycle 13. Nevertheless, the chromosomes exhibit characteristic condensation of their heterochromatic material, an event that normally occurs only during cellularization at nuclear cycle 14 in wild-type embryos (Sonnenblick, 1950).

The formation of larva and adults from the dal*-derived embryos*

All of the *dal*-derived late blastoderm embryos exhibit major abnormalities in their surface nuclear distribution, and they also have an unusually large fraction of their nuclei in the interior of the embryo at cellular blastoderm. Nevertheless, these embryos continue developing – with many progressing to late embryogenesis and even adulthood. We have examined cuticle preparations of those *dal*-derived embryos that remain unhatched after 40 h of development. These display defects that vary in their degree of severity; for example, of 83 unhatched embryos, 54 % completely lacked cuticular structure, 30 % had an otherwise normal cuticle with fused segments, and 13 % had a cuticle with very disorganized patterns including holes in the cuticular structure.

In view of the severe nuclear abnormalities seen at cellular blastoderm, it is perhaps surprising that about 8 % (104/1254) of the *dal*-derived embryos develop to adulthood. Nomarski photographs of living *dal*-derived embryos have been used to show that individuals that cellularize at one-half of the normal nuclear density can nevertheless develop into an adult (data not shown). Inspection of these adults reveal that 5 to 10 % miss an entire wing or leg and that a much higher frequency possess abnormally arranged tergites. These surviving adults are assumed to represent escapers that were able to compensate for their severe deficiency of cells at gastrulation – although not without frequent errors in their developmental pattern. The wild-type allele of *dal*, which is capable of a partial paternal rescue, was present in these embryos, being supplied paternally (Sullivan, 1987).

Interestingly, Zalokar and Erk (1975) have described

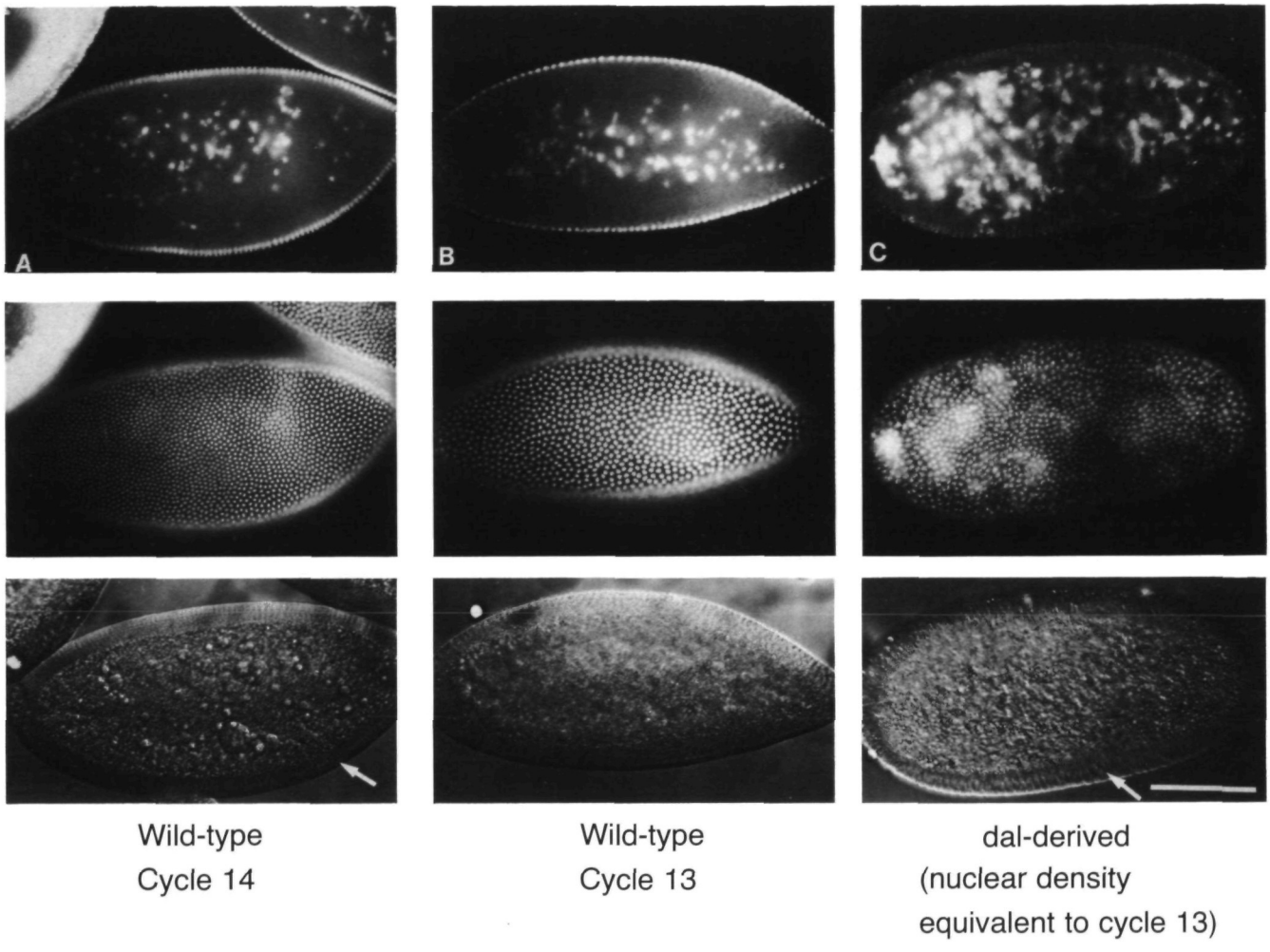

Fig. 1. The *dal*-derived embryos cellularize at one-half of the normal nuclear density and exhibit extra internal nuclei. The top and middle rows depict interior and surface views, respectively, of the nuclei in DAPI-stained embryos (a fluorescent DNA stain). The bottom row shows Nomarski images highlighting the cellularization furrows of the embryos (the arrows in the Nomarski images of columns A and C mark the furrows). Column A shows a normal cellularized cycle 14 embryo; column B shows a normal non-cellularized cycle 13 embryo; column C shows a cellularized *dal*-derived embryo. Notice that the cellularized *dal*-derived embryo has a nuclear density similar to that of a non-cellularized normal cycle 13 embryo. The *dal*-derived embryo also has a great excess of internal nuclei (compare A with C in top row). Bar, equals 0.1 mm.

an X-linked maternal-effect mutation that results in the production of embryos with an excess of internal nuclei, and these also produce flies with missing legs.

The early dal*-derived embryo develops normally through nuclear cycle 10*

Nuclear migration outward from the interior of the embryo normally begins during telophase of nuclear cycle 8 and ends when the nuclei reach the plasma membrane during interphase of cycle 10 (Foe and Alberts, 1983). About fifty of the nuclei are left behind. These internal 'yolk nuclei' divide in cycles 9 and 10 in close synchrony with the peripheral nuclei and then undergo several rounds of DNA replication without accompanying nuclear division (Foe and Alberts, 1983). When zero to three hour egg collections from homozygous *dal* females were fixed and their nuclei stained with DAPI, no gross irregularities were detected during nuclear cycles 8, 9 and 10 with respect to the arrangement and number of either migrating or surface nuclei (Table 1). Moreover, the amount of developmental time required for embryos derived from *dal*- females to reach nuclear cycle 10 (the completion of nuclear migration) differs by at most five minutes from normal, an insignificant variation. In addition, the number of internal yolk nuclei in *dal*-derived cycle 10 embryos is normal.

To establish control values for our studies to be described below, we scored the surface nuclei on 17 formaldehyde-fixed wild-type embryos between nuclear cycles 10 through 13 (we could examine approximately one-half of the nuclei in each embryo). Six of the 17 embryos had one or more visible nuclear defects. In all, we scored 8346 nuclei and recorded 18 defects (16 irregularly shaped nuclei and 2 holes on the surface lacking nuclei, representing a value of 0.2% irregularities. Frequencies of nuclear defects in this range are therefore considered normal.

Table 1. *The phenotype of* dal-*derived DAPI stained embryos plotted with respect to nuclear cycle*

Cell cycle estimated by nuclear density	8	9	10	11	12	13	13 (cells)
Normal nuclei	5 100%	21 100%	14 100%	8 32%	1 3%		
Bridges between nuclei uneven nuclear spacing				14 56%	14 37%	2 5%	
Bridges, uneven spacing and nuclei in the cortical cytoplasm				3 12%	13 34%	13 32%	
Bridges, uneven spacing nuclei in cortical cytoplasm and extra yolk nuclei					10 26%	22 54%	3 14%
Normal peripheral nuclei nuclei in cortical cytoplasm and extra yolk nuclei						4 10%	6 27%
Normal peripheral nuclei no nuclei in cortical cytoplasm and extra yolk nuclei							13 59%

166 *dal*-derived DAPI-nuclear stained embryos were scored both in terms of their surface and internal nuclei. Their nuclear cycle was estimated from nuclear density counts on each embryo. The values represent the number of embryos with the nuclear density and the nuclear phenotype indicated by that row and column.

The first nuclear irregularities in dal-*derived embryos occur during cycle 11*

Of 25 *dal*-derived embryos examined at cycle 11, 8 appeared normal with respect to their surface and internal nuclei, whereas 14 had nuclei of irregular shape and size on their surface. These nuclei appeared to result from either an incomplete separation of daughter nuclei or a fusion of two nuclei. Many of them stained much brighter with DAPI than the surrounding nuclei, suggesting that they contain more than the diploid amount of DNA. Moreover, in wild-type embryos the cortical cytoplasm just beneath the surface monolayer does not contain nuclei after cycle 10. However, 3 of the 25 *dal*-derived embryos had nuclei in this region of the cortical cytoplasm (Fig. 2 and Table 1).

Cycle 12 embryos have a high frequency of peripheral nuclear abnormalities and also an excess of interior nuclei

Of 38 *dal*-derived embryos examined at cycle 12, 37 exhibited the same types of nuclear abnormalities on their surface seen in cycle 11 embryos. However, the abnormalities were more numerous and involved larger regions. In addition, a much higher fraction (23/38) of cycle 12 embryos had nuclei in the region of the cortical cytoplasm that is normally nuclear-free, and large patches without nuclei were seen on the surface of the embryos. Finally, 10 of these embryos had, in addition to the above features, a marked excess of internal nuclei as compared to wild-type embryos at the same stage (Fig. 2, Table 1). In 11 embryos derived from *dal/Cy* females and 15 embryos derived from *dal/dal* females we measured the ratio of the area taken up by the internal nuclei relative to the total area of a medial section of the embryo (see Materials and methods). The values for syncytial embryos derived from *dal/Cy* females ranged from 0.05 to 0.07 and the values for the equivalent *dal/dal* females were frequently above 0.20.

Older dal-*derived embryos have a large excess of internal nuclei*

As will be demonstrated later, the products of aberrant peripheral nuclear divisions eventually sink inward and leave the surface monolayer. Much of this loss of surface nuclei occurs just prior to cellular blastoderm, which makes it impossible to distinguish clearly between cycle 13 and cycle 14 *dal*-derived embryos by nuclear density counts.

Of the 41 *dal*-derived embryos examined prior to cellularization with a nuclear density equivalent to a normal nuclear cycle 13 (some in cycle 13 and some just prior to cellularization in cycle 14), none appeared normal. Two of 41 had abnormal surface nuclei with no other obvious defects. Thirteen of 41, in addition, had nuclei at an abnormal depth in the cortical cytoplasm. Twenty-two of 41 had, in addition to the above two types of abnormalities, many extra internal nuclei; this class occurred with about double the frequency (22/41) observed for cycle 12 embryos. Finally, a new class of embryos first appears in embryos with a cycle 13 nuclear density: 4 of 41 had both extra internal nuclei and nuclei at an abnormal depth in the cortical cytoplasm but no irregularity in their surface nuclei (Fig. 2, Table 1); we believe that these are the embryos that have recently entered cycle 14 (see below).

The *dal*-derived embryos that have begun cellularizing can be detected by the membrane furrows that become clearly visible in Nomarski images. At this stage, one observes a high frequency of embryos with normal surface nuclei (19/22) as compared to the situation in slightly younger embryos with a similar nuclear density, where only 4/41 appeared normal in this respect. In addition, in many of the cellularizing

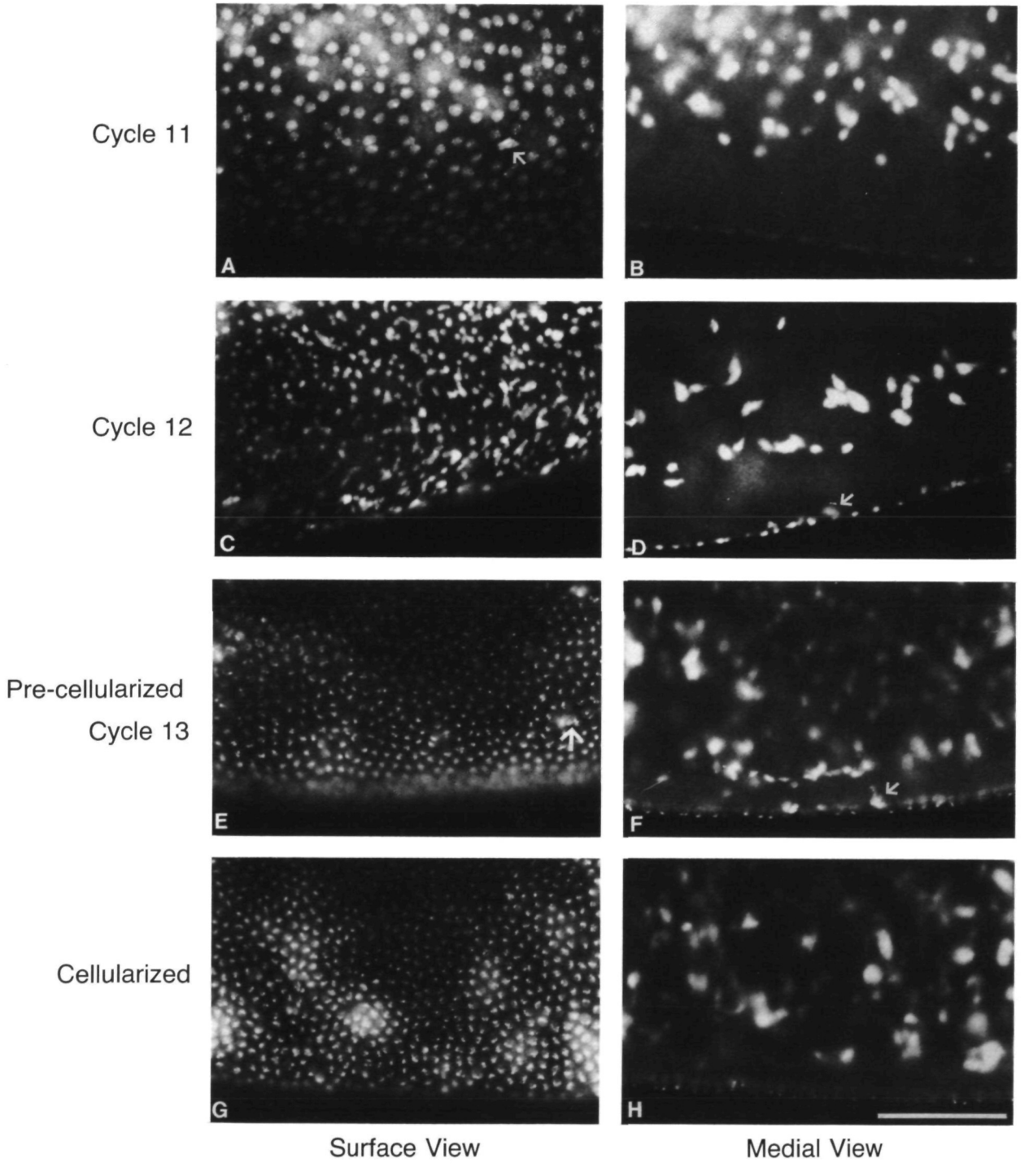

Fig. 2. Nuclear behavior in *dal*-derived embryos from nuclear cycle 11 to cellularization (cycle 14). In each pair of photographs, the same DAPI-stained, fixed embryo is viewed in a surface focal plane (left) and an interior focal plane (right). Bar, equals 0.05 mm. (A,B) During nuclear cycle 11, *dal*-derived embryos exhibit a few irregularly shaped and spaced surface nuclei (see arrow in A). The internal yolk nuclei appear normal (B). (C,D) During nuclear cycle 12, a much higher frequency of abnormal nuclei are observed on the surface (C). In addition, nuclei are seen in the cortical cytoplasm (arrow in D), just below the monolayer of peripheral nuclei (in wild-type embryos this zone is free of nuclei after cycle 10). (E,F) An embryo just prior to cellularization. This embryo has a nuclear density on the surface equivalent to that of a wild-type nuclear cycle 13 embryo, with only a few irregularities (arrow in E). There is a large excess of internal nuclei as well as nuclei present in the cortical cytoplasm (arrow in F). (G,H) A cellularized embryo has a surface that is free of defects (G), but a vast excess of interior nuclei (H).

embryos (13/22), the cortical cytoplasm is clear of abnormal nuclei so that the border between the cortical and the internal cytoplasm is clearly defined by the outermost position of the excess internal nuclei (Fig. 1, top panel, column C).

In summary, the *dal*-derived embryos develop normally until nuclear cycle 10. During nuclear cycle 11, a small fraction of the nuclei just beneath the embryo surface undergo mitotic irregularities that result in abnormally shaped and sized nuclei. A greater proportion of such irregularities appear during nuclear cycle 12, and, in addition, nuclei are seen in the cortical cytoplasm unusually far from the plasma membrane in most embryos. Extra nuclei located more internally in the embryo also appear for the first time. At a surface nuclear density equivalent to nuclear cycle 13, almost all embryos have more internal nuclei than normal. This data can be explained if the nuclei that divide abnormally leave the surface and sink through the cortical cytoplasm into the interior of the embryo. As judged by time-lapse recordings of live embryos, the *dal*-derived nuclei on the surface – like their wild-type counterparts – cellularize shortly after the mitosis that begins cycle 14 (see below). However, because of the large number of nuclei lost to the inside of the embryo, cellularization occurs at a surface nuclear density that is only about half the wild-type value (Fig. 2, Table 1).

The centrosomes of *dal*-derived embryos were immunofluorescently visualized with an antibody that allows us to follow centrosome behavior (see Materials and methods). Areas that contain abnormal nuclei (as judged by DAPI staining) in *dal*-derived embryos also have centrosomes of abnormal size and spacing near their surface. In addition, the areas on the surface with no nuclei, which become common during the late syncytial divisions, contain an unusually high concentration of centrosomes. Often, more internally positioned nuclei can be seen directly below these centrosome-enriched patches. In fact, the areas of most intense centrosomal staining correspond to the regions in the embryo that have DAPI-staining nuclear material in the normally nuclei-free portion of the cortical cytoplasm. Thus, nuclei that have undergone an abnormal division appear to sink into the center of the embryo and leave their centrosomes on the surface. The real-time analysis in the next section will demonstrate these points more directly.

In vivo *analysis with fluorescently-labeled histones reveals the types and frequencies of mitotic defects*

The injection of fluorescently labeled histones into *dal*-derived embryos enables one to follow the nuclear divisions using fluorescence microscopy and image processing (Minden *et al.* 1989). Fig. 3 shows a series of live images of a region of a single embryo from telophase of cycle 10 through interphase of cycle 12 that experiences the two types of mitotic abnormalities commonly observed in *dal*-derived embryos: (1) division failures: the nucleus marked with an arrowhead in panels A–E fails to divide at the end of cycle 11; in panel F, this nucleus disappears from the surface plane leaving an empty region; (2) the fusion of two neighboring nuclei at telophase: in panel E and F, one of the mitotic products from the nucleus marked with an arrow in panels A–H and one of the products from the nucleus marked with an inverted V fuse during telophase of cycle 11.

Table 2. *Frequency and types of nuclear abnormalities occurring in* dal*-derived embryos at each nuclear cycle*

Mitosis of	Normal	Nuclear division phenotypes: Telophase fusion	Nuclear division phenotypes: Division failure	% Abnormal divisions
cycle 10	164 (104)	0	4 (2)	2.3% (1.9%)
cycle 11	656 (242)	14	61 (3)	10.3% (1.2%)
cycle 12	233 (182)	46	35 (3)	28.7% (1.6%)
cycle 13	96 (96)	8	6 (0)	12.7% (0.0%)

Using time-lapse video-microscopy and fluorescently labeled histones, we were able to follow two *dal*-derived embryos through four mitotic divisions (9 through 13). At the interphase of each cycle, 20 to 50 nuclei were selected and followed to the interphase of the next cycle. The selection of the nuclei to be followed was random with the exception that nuclei that had previously undergone an abnormal division were not included in the counts. All of the progeny of an abnormal nucleus divion will produce only abnormal nuclei that will be lost from the surface.

Our studies with labeled histones demonstrate directly that *dal*-derived embryos undergo 13 mitotic divisions and cellularize during nuclear cycle 14, as do normal embryos. In addition, following the nuclei in live embryos, we have been able to score the frequencies of each type of mitotic defect as a function of embryo age. The results are presented in Table 2. During nuclear cycle 10, the few division abnormalities observed were at the same level as the control values for wild-type embryos. However, of 731 nuclear division products examined during cycle 11, 14 experienced telophase fusions and 61 experienced division failures. The fraction of abnormal divisions reached a maximum in cycle 12, when nearly 30% of the divisions were abnormal. A nucleus has a 50% probability of undergoing an abnormal division during cycles 11 through 13, and these are lost from the surface monolayer of nuclei before the time of cellularization. This accounts for our observation that most *dal*-derived embryos cellularize at about one-half of the normal nuclear density.

The technique used in Fig. 3 does not allow us to follow the fate of the abnormal nuclei that drop into the interior of the embryo. We therefore do not know whether they undergo additional divisions or become polyploid. In addition, although we know that many of the extra internal nuclei in *dal*-derived embryos arise from the abnormal surface nuclei sinking inward, we cannot rule out the possibility that some of these excess

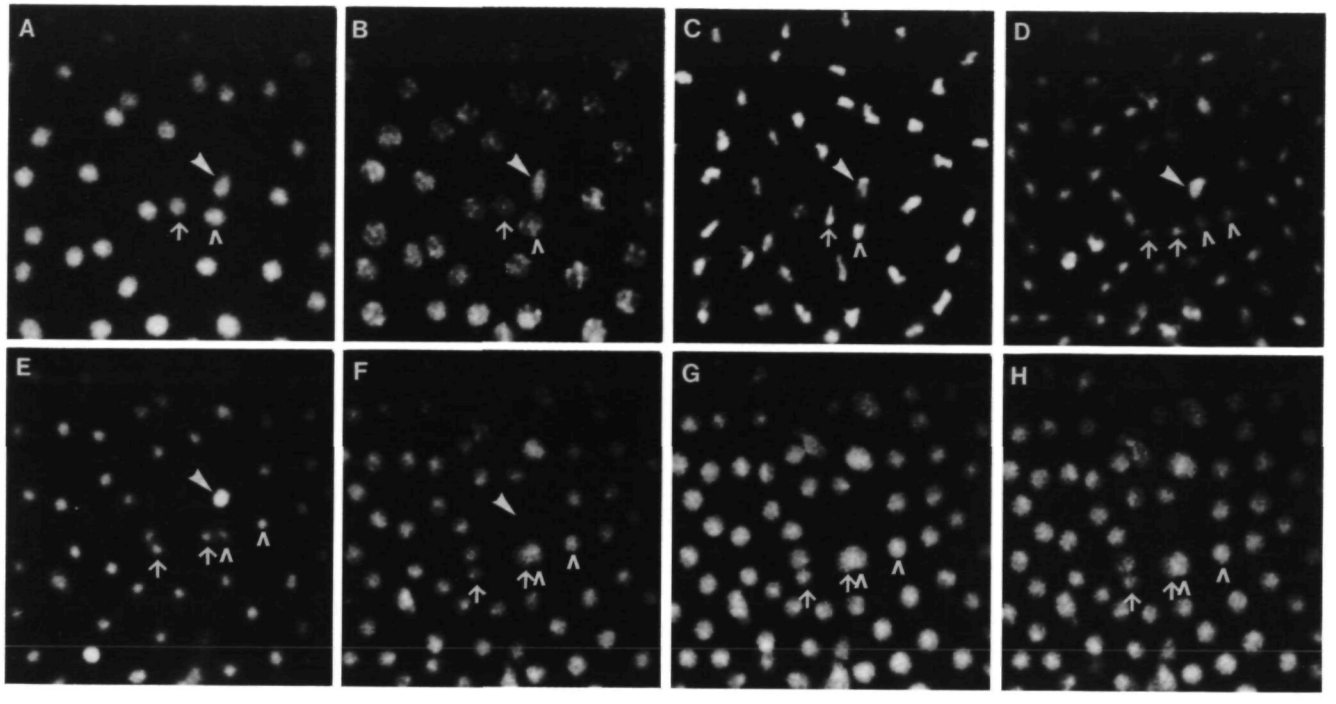

Fig. 3. Photographs of a *dal*-derived embryo injected with fluorescently labeled histones. This *dal*-derived embryo was followed from telophase of nuclear cycle 10 (A) to the interphase of nuclear cycle 12 (H). The arrow, arrowhead, and V trace the behavior of three nuclei. Panels B,C,D, and E depict interphase, metaphase, anaphase and telophase of nuclear cycle 11, respectively. The nucleus marked by the arrowhead fails to separate its chromosome complements during anaphase (D). During the telophase/interphase transition that begins nuclear cycle 12, two of the neighboring mitotic division products fuse (nuclei marked by an arrow and a V in panel F). The nucleus that failed to divide sinks inward out of the focal plane during the interphase of nuclear cycle 12 (F and G; arrowhead in A–F).

internal nuclei result from extra divisions of true yolk nuclei.

In vivo *analysis with fluorescently labeled tubulin reveals that many centrosomes fail to separate normally in* dal*-derived embryos*

The microtubules can be continuously monitored during the syncytial embryonic divisions in *Drosophila* by injecting embryos with fluorescently labeled tubulin (Kellogg *et al.* 1988). Since centrosomes serve as prominent microtubule-organizing centers, we have followed the centrosome cycle in this way in *dal*-derived embryos (Fig. 4). Such an analysis demonstrates that many centrosomes either completely or partially fail to separate during the syncytial divisions in these mutant embryos. If the nucleus with incomplete centrosome separation has no close neighboring nuclei, no functional spindle is formed (Fig. 4, D–F). However, many of the nuclei with incompletely separated centrosomes become closely associated with a neighboring nucleus, which allows a normally separated centrosome from the neighboring nucleus to associate with the defective nucleus, as well as with its own nucleus. In the following metaphase, this shared centrosome will serve as a common pole for the spindles of both nuclei (Fig. 4, A–C).

In order to determine the consequences of this abnormal centrosome behavior for chromosome separation, we have injected *dal*-derived embryos with a mixture of NHSR-labeled histones and NHSF-labeled tubulin. The types and frequencies of abnormal nuclear behavior observed in the doubly injected embryos are equivalent to those observed in both the fixed and the singly injected embryos. Fig. 5 depicts the consequences of abnormal centrosome separation during interphase. Frequently, one of the centrosomes of a neighboring normal nucleus serves as a pole for both its own nucleus and the spindle formed by the nucleus with an unseparated pair of centrosomes. As a result, during anaphase two sets of chromosomes are pulled to a single pole, where they coalesce to form a single nucleus during telophase (from other examples, we know that the fusion can occasionally occur later in the following interphase). Fig. 5 also exhibits two instances of failed centrosome separation in which the centrosomes of a neighboring nucleus were not close enough to contribute a pole. In these cases, no spindle was formed and the nucleus with unseparated centrosomes did not divide.

From experiments like that shown in Fig. 5, we have classified all of the nuclear division defects observed during nuclear cycles 11 and 12 with regard to centrosome behavior (Table 3). Division failures were the only defect found when either a shortened spindle or no spindle formed with no sharing of centrosomes between nuclei. All of the abnormal spindle complexes connecting adjacent nuclei observed were the result of a

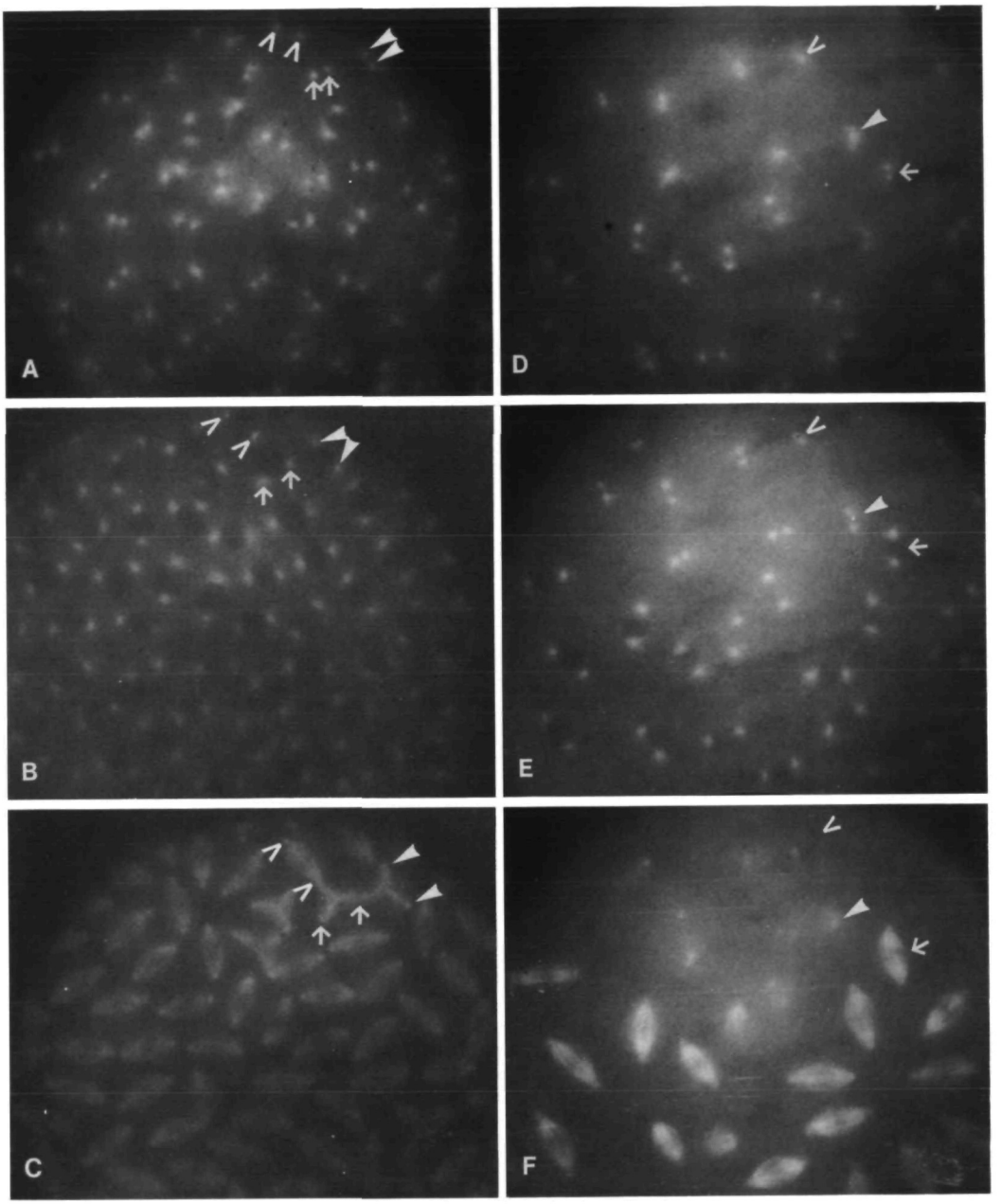

Fig. 4. *In vivo* analysis of *dal*-derived embryos with fluorescently labeled tubulin. Two *dal*-derived embryos were followed – one from interphase to metaphase of cycle 12 (A–C) and the other from interphase to metaphase of cycle 11 (D–F). In both cases, the arrowhead, arrow and V follow the sister centrosomes of three nuclei. Panels A–C show what happens when centrosomes interact between neighboring nuclei. In panel A, the centrosomes are just beginning to separate. In panel B, the sister centrosomes marked by the V have completely separated and the two centrosomes are on opposite sides of the nucleus; in contrast, the other two centrosome pairs have not completely separated and remain more on one side of the nucleus than the other. In addition, two of the centrosomes are each associated with two nuclei (rightmost centrosomes of the centrosome pairs marked by the arrow and the V). This often occurs when one of the nuclei involved has incompletely separated centrosomes, but is otherwise never seen. The metaphase configuration (panel C) demonstrates that the shared centrosomes form an abnormal dual spindle. Panels D–F demonstrate the effects of failed and incomplete centrosome separation in those cases where the abnormal centrosomes fail to interact with a second neighboring nucleus. While the nucleus marked by the arrow has completely separated its centrosomes in panel D, the other two nuclei have failed to separate (V) or only partially (arrowhead) separated their centrosomes. Panels E and F show that these latter nuclei fail to make a spindle.

single centrosome associating with two nuclei and serving as a spindle pole for two nuclei simultaneously. In some of these cases, a nucleus failed to divide despite its sharing of a spindle. However, often telophase fusions of nuclei and unequal divisions occurred. In total, 11 of the 13 nuclear fusion events observed were

Table 3. *Analysis of* dal*-derived embryos co-injected with rhodamine-labeled histones and fluorescein-labeled tubulin*

Cycle 11			
	Single spindle (n=90)		
Normal	Fusion	Nondivider	Unequal
83	0	7	0
	Multiple spindles (n=26)		
Normal	Fusion	Nondivider	Unequal
6	6	11	3
Cycle 12			
	Single spindle (n=58)		
Normal	Fusion	Nondivider	Unequal
53	0	5	0
	Multiple spindles (n=35)		
Normal	Fusion	Nondivider	Unequal
10	20	4	1

The centrosome, spindle and chromatin behavior were simultaneously followed from early interphase through telophase of nuclear cycle 11 (4 embryos observed) or from early interphase through telophase of nuclear cycle 12 (3 embryos observed) by filming embryos injected with both fluorescein-labeled tubulin and rhodamine-labeled histones. The number listed refers to the total number of nuclei of each type observed in these experiments. Multiple spindles result from a single centrosome interacting with two neighboring nuclei at prophase and serving as a pole for two spindles. All other spindles were scored as single. As described in the text, the histones reveal three types of defects; nuclear division failures, fusion during late telophase or early interphase and unequal partitioning of the chromosomes at anaphase.

the result of a single centrosome pulling the chromosomes from two nuclei to a single pole. In the other two cases, nuclear fusion occurred from incomplete centrosome separation leading to two centrosomes lying so close to one another that they functioned as a single centrosome. Tripolar spindles resulted from one normal centrosome interacting with a neighboring nucleus in which the partially separated centrosomes were far enough apart so that each nucleated a separate array of microtubules. The chromatin associated with these spindles often separated unevenly at anaphase.

The closer spacing of nuclei in cycle 12 gives rise to a higher frequency of multiple spindles (spindles with a shared spindle pole) than in cycle 11 (Table 3), which accounts for the increased error frequency in the later cycle.

The above types of centrosome abnormalities will often produce a nucleus with multiple centrosomes in the next interphase. When these centrosomes subsequently replicate, one or more of the replicated products usually loses its association with the nuclear envelope and migrates away from the nucleus but remains in the cortical cytoplasm. For instance, in Fig. 5E–H, the sister centrosomes in four nuclei with shared centrosomes migrate away from the nuclear envelope into the cytoplasm. This observation accounts for the free centrosomes observed on the surface of fixed *dal*-derived embryos.

Of 15 nuclei that failed to divide during cycle 11, 4 sunk inward during the next cycle and 2 migrated in and out of the focal plane – indicating they had lost their normal cytoskeletal connections. Normarski recordings reveal that many (if not all) of the remaining aberrant nuclei will sink inward during the early stages of cellularization in nuclear cycle 14.

Discussion

The *dal* maternal-effect mutation affects nuclear division primarily during the late blastoderm divisions. The *dal*-derived embryos divide normally through nuclear cycle 10. During nuclear cycles 11 through 13, however, these embryos exhibit a high frequency of division failures, telophase fusions and unequal chromatin separation. However, the embryos are capable of relatively normal development after cellular blastoderm. The *dal* mutation has been described as a hypomorph (Sandler, 1977), and one explanation for this phenotype is that the *dal*-derived embryo, with a reduced amount of maternally supplied wild-type *dal* product, cannot support proper nuclear division after nuclear cycle 10.

Alternatively, the *dal*-product may be required only for the peripheral blastoderm divisions that occur after nuclear migration. During nuclear cycle 8 in a normal embryo, all but about fifty of the nuclei start to migrate to the periphery of the embryo. The fifty that remain behind are on a different division program than the nuclei that migrate to the periphery. These internal nuclei undergo two more divisions in approximate synchrony with the peripheral nuclei, but later they increase in size – presumably undergoing DNA replication during cycles 10–13 without accompanying nuclear division (Zalokar and Erk, 1976; Foe and Alberts, 1983). These different division programs may result from the presence of different maternally supplied components in the cortical and internal cytoplasm. If the *dal*-derived embryos are defective in a component necessary only in the later cortical nuclear divisions, the abruptness of the shift of the *dal*-derived embryos to abnormal divisions in cycle 11 could be easily explained. Distinguishing among the various possibilities for the wild-type function of *dal*, however, will probably require the isolation of null alleles and the cloning of the gene.

Raff and Glover (1988) have examined embryos injected with aphidicolin, an inhibitor that blocks DNA replication. Although nuclear division is prevented by the injection, the centrosomes dissociate from the nucleus, continue replicating, and in some instances migrate to the surface of the embryo. In *dal*-derived embryos, the reciprocal phenomenon occurs; some of the surface nuclei migrate inward, leaving their centrosomes behind on the surface. Whereas the outward migration requires microtubules and the centrosome, the inward migration of the aberrant nuclei appears to be independent of the centrosomes. We have not followed the division behavior of these nuclei once they reach the interior of the embryo, although they are very unlikely to divide since they lack centrosomes.

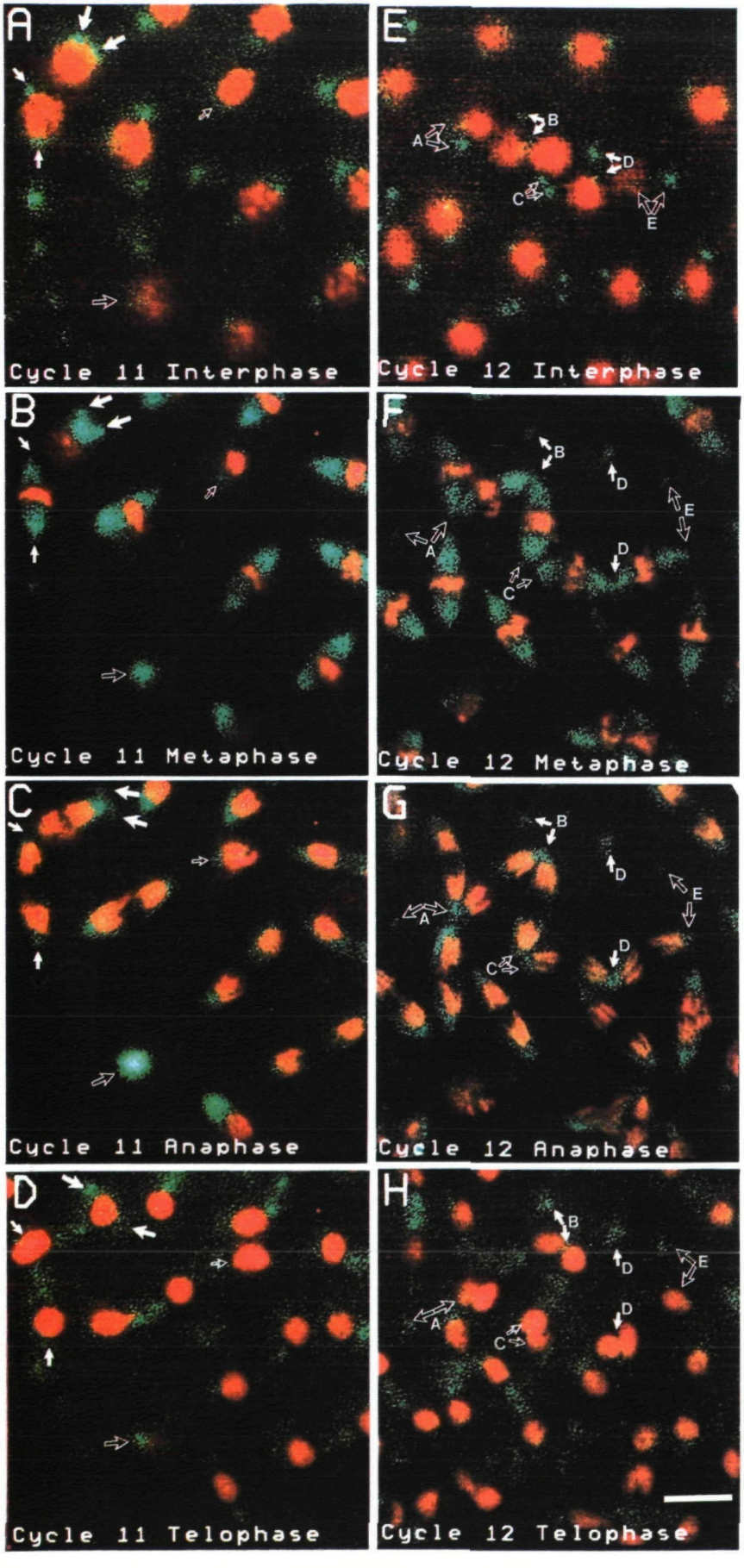

Fig. 5. A *dal*-derived embryo injected with fluorescein-labeled tubulin (green) and rhodamine-labeled histones (red). Bar, equals 0.01 mm. (A) Cycle 11 interphase; the arrows indicate the position of the centrosomes. The smaller pair of solid arrows indicates a centrosome pair that has separated completely. The larger pair of solid arrows indicates a centrosome pair that has duplicated but failed to separate normally. The two open arrows indicate nuclei in which the centrosomes have either failed to separate or failed to duplicate. (B) Cycle 11 metaphase; the arrows mark the centrosomes described in A. The nuclei with no centrosome separation (indicated by the open arrows) fail to form a spindle. The centrosome marked by the uppermost small solid arrow is interacting with the neighboring nucleus in which the centrosomes have failed to separate normally. This centrosome will serve as a common pole for the metaphase spindles of the two nuclei (see C and D below). (C) Cycle 11 anaphase; the nuclei that failed to form a spindle in B (open arrows) fail to divide. The nucleus marked by the larger open arrow that failed to divide has sunk below the focal plane. The nucleus marked by the two large solid arrows has formed a spindle and is separating its chromatin because the centrosome from the neighboring nucleus has served as a second pole (smaller solid arrow). Two sets of chromatin are being pulled toward this shared pole. (D) Cycle 11 telophase; the chromatin from two separate nuclei pulled to a common pole fuses in telophase (uppermost small solid arrow) (E) Cycle 12 interphase; the sets of paired arrows depict five centrosome pairs that have failed to separate. One centrosome from each pair appears to be free of the nuclear membrane. (F) Cycle 12 metaphase; the centrosomes that remain attached to the nucleus also associate with the nucleus of a neighbor. As a result, each of these centrosomes serves as a common spindle pole for two nuclei. The unattached sister centrosomes have migrated into the cytoplasm. In one instance, however, the free centrosome has associated with a neighboring nucleus and functions as a spindle pole for that nucleus (C, right arrow) (G) Cycle 12 anaphase; the chromatin can be seen being pulled to a common pole in those instances in which a centrosome is shared between two nuclei. (H) Cycle 12 telophase; telophase fusions result from chromatin being pulled to a common pole. In one instance, even though the chromatin was being pulled to a common pole fusion did not occur (B). In another case, a telophase fusion occurred when the chromatin was being pulled to two separate poles that were so closely associated that they effectively served as one (C).

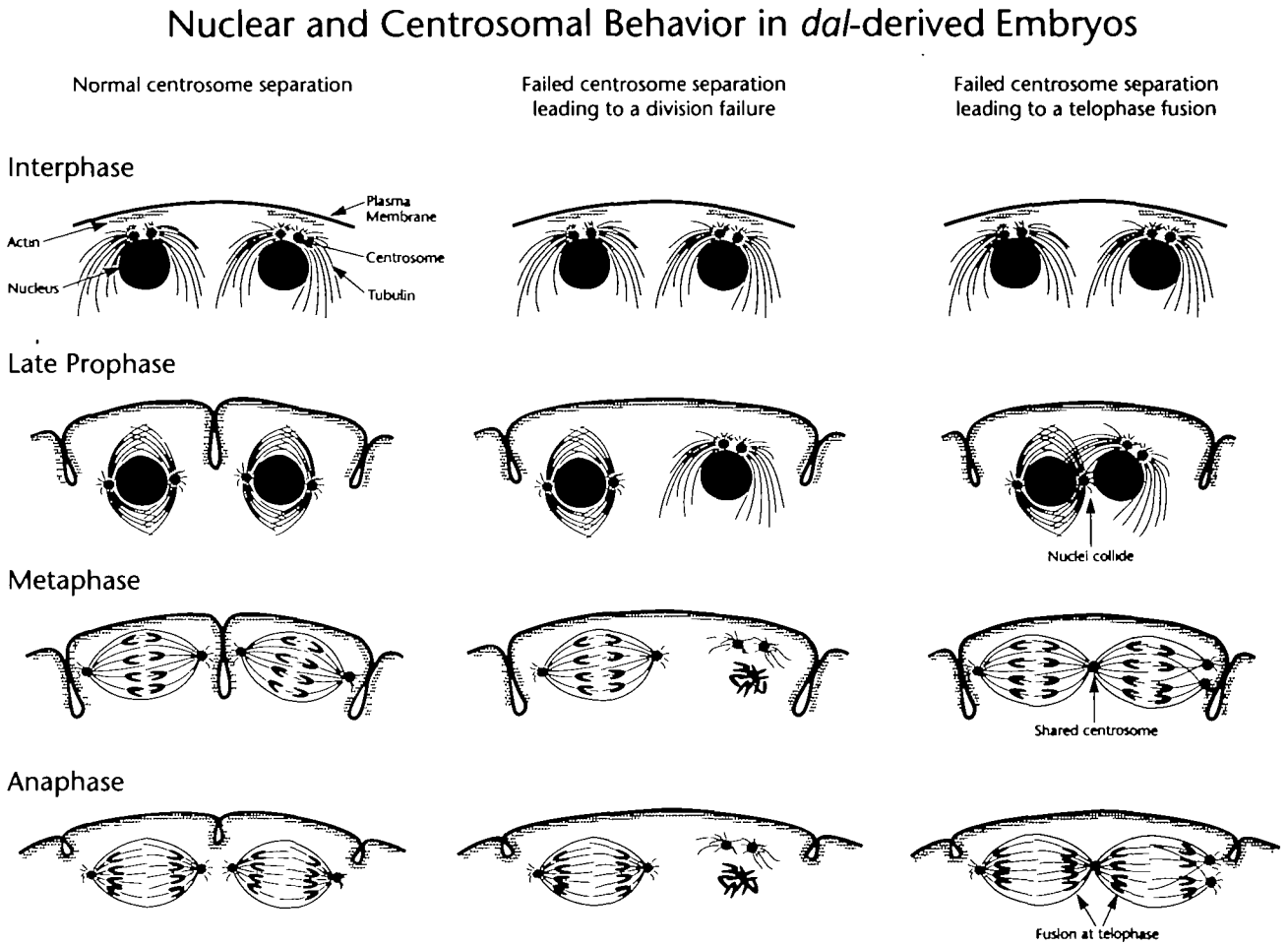

Fig. 6. Schematic illustration of the consequences of centrosome failure in *dal*-derived embryos that suggests an important role for the pseudocleavage furrows during the syncytial nuclear divisions. Failed centrosome separation in *dal*-derived embryos results in either division failures or telophase fusions. The latter result from two nuclei colliding and sharing centrosomes. We propose that the failure of the centrosomes to separate prevents the actin-based pseudocleavage furrows from being properly formed (see text). Without these furrows, the nuclei do not remain in separate domains and they therefore collide frequently.

Minden *et al.* (1989) have shown that the products of a rare abnormal nuclear division observed in wild-type embryos will also sink inward. Similarly, Warn *et al.* (1987) have reported that, after an injection of an antibody to tubulin, the spindles collapse and the associated nuclei sink inward leaving their centrosomes on the surface. In addition, we have injected antibodies to a protein distributed in a ring-like manner outside of the nuclei of the *Drosophila* embryo. These injections disrupt nuclear division, and the abnormal nuclei migrate inward (unpublished results of W.S.). It therefore appears that the *Drosophila* embryo somehow responds to abnormal cortical nuclei by allowing them to fall inward. During syncytial and cellular blastoderm, important nuclear–nuclear and cell–cell interactions occur in the surface monolayer of nuclei (Ingham, 1988). The loss of the products of abnormal mitotic divisions to the interior of the embryo may have evolved to help protect these surface interactions (Sullivan, 1987).

We propose that the abnormal nuclear divisions observed in the *dal*-derived embryos is a direct consequence of a failure of the centrosomes to separate properly (see Fig. 6). In these embryos, some 10 to 30% of the nuclei during cycles 11 through 13 either partially or completely fail to separate their centrosomes during interphase. Consequently, a shortened spindle or no spindle forms and this results in a division failure. Often, however, the centrosome of a neighboring nucleus associates with a nucleus with incompletely separated centrosomes. This centrosome associates with two nuclear membranes and can serve as a spindle pole for both nuclei in the following mitosis. Two sets of chromatin can then be pulled to a single pole at anaphase, accounting for the observed telophase fusions of nuclei. The frequency of telophase fusions is greater in nuclear cycle 12 than in cycle 11, reflecting the closer spacing of the nuclei in the later cycle and, therefore, the greater the chance of a neighboring nuclei sharing its centrosome. Nuclei with partially separated centrosomes are very often closely associated with a neighboring nucleus. We therefore suggest that

the cytoplasmic domains that normally keep the nuclei spaced apart (see Karr and Alberts, 1986) are defective unless the centrosomes separate normally.

Why do nuclei collide only with those nuclei whose centrosomes have failed to separate? We suggest that the basis of this phenomenon is the improper formation of pseudocleavage furrows (see Fig. 6). During prophase of cycles 11, 12 and 13, these actin-based membrane furrows pull down around each nucleus as mitosis begins, so that each metaphase spindle is surrounded by these furrows (Stafstrom and Staehelin, 1984). Rappaport (1971) has argued that, during a normal mitosis, cleavage furrows form between the two asters of the same spindle in a plane perpendicular to the spindle axis. Stafstrom and Staehelin (1984) have proposed that a similar mechanism may be operating in the formation of the pseudocleavage furrows of the *Drosophila* embryo, except that they form wherever the centrosomes of adjacent spindles are close to one another.

It is significant that, in *dal*-derived embryos, the nucleus whose centrosomes have failed to separate collides with a neighboring nucleus on the side farthest away from the unseparated centrosomes (see Fig. 6). This makes sense if we assume that pseudocleavage furrows can form only when the centrosomes from two neighboring nuclei come close to each other, and that it is the furrow-forming mechanism that normally keeps mitotic nuclei apart during cycles 11 to 13.

While in many organisms there is a correlation between chromosome content and both nuclear and cell size (Cavalier-Smith, 1982), it appears this is not the case for *Drosophila* embryos (Zussman and Wieschaus, 1987). Thus, when *dal*-derived blastoderm embryos cellularize, the nuclei and cells are much larger than those of a wild-type cycle 14 embryo, even though they are likely to have normal DNA content. In these embryos, the nuclei seem to expand to fill up the available surface area, as they presumably also do during normal development (Foe and Alberts, 1983).

The cellularization of *dal*-derived embryos at half the normal nuclear density suggests that cellularization in *Drosophila* embryos is not directly linked to nuclear density. In *Xenopus*, there is evidence for a nuclear/cytoplasmic titration mechanism controlling the mid-blastula transition (Newport and Kirschner, 1982). Edgar *et al.* (1986) have found similar results for the *Drosophila* embryo. The lengths of nuclear cycles 10 through 14 in *dal*-derived embryos are equivalent to wild-type values (data not shown). If the nuclear/cytoplasmic titration mechanism proposed by Edgar *et al.* (1986) occurs, the behavior of the *dal*-derived embryos suggest that the aberrant nuclei that sink into the interior of the embryo are competent to titrate the cytoplasmic factors.

This work is dedicated to the memory of Larry Sandler. We would like to thank Tom Kornberg and Glenn Yasuda for their critical readings of the manuscript. Also, we thank the members of the Alberts, Schubiger and Wakimoto laboratories for their helpful advice. We are especially grateful to John Sedat and David Agard, and the Howard Hughes Medical Institute for their advice and generously allowing us to use their microscope and computer facilities. Finally, we would like to give special thanks to Douglas Kellogg for generously providing us with the labeled tubulin, technical expertise, and critical comments on all aspects of this work.

This work was supported in part by National Institutes of Health grant GM31286 to Bruce Alberts. William Sullivan and Jonathan S. Minden were supported by fellowships from the Helen-Hay Whitney Foundation.

References

AGARD, D. A., HIROAKA, Y., SHAW, P. AND SEDAT, J. W. (1988). Fluorescent microscopy in three dimensions. *Methods Cell Biology* **30**, 353–377.

CAVALIER-SMITH, T. (1982). Skeletal DNA and the evolution of genome size. *A. Rev. Biophys Bioeng.* **11**, 273–302.

EDGAR, B. A., KIEHLE, C. P. AND SCHUBIGER, G. (1986). Cell cycle control by the nucleo-cytoplasmic ratio in early *Drosophila* development. *Cell* **44**, 365–372.

EDGAR, B. A. AND O'FARRELL, P. H. (1989). Genetic control of cell division patterns in the *Drosophila* embryo. *Cell* **57**, 177–187.

FOE, V. E. AND ALBERTS, B. M. (1983). Studies of nuclear and cytoplasmic behavior during the five mitotic cycles that precede gastrulation in *Drosophila* embryogenesis. *J. Cell Sci.* **61**, 31–70.

FREEMAN, M. AND GLOVER, D. M. (1987). The *gnu* mutation of *Drosophila* causes inappropriate DNA synthesis in unfertilized and fertilized eggs. *Genes and Development* **1**, 924–930.

FREEMAN, M., NUSSLEIN-VOLHARD, C. AND GLOVER, D. M. (1986). The dissociation of nuclear and centrosomal division in *gnu*, a mutation causing giant nuclei in *Drosophila*. *Cell* **46**, 457–468.

GATTI, M. AND BAKER, B. S. (1989). Genes controlling essential cell cycle functions in *Drosophila melanogaster*. *Genes and Development* **3**, 438–453.

GONZALES, C., CASAL, J. AND RIPOLL, P. (1988). Functional monopolar spindles caused by mutation in mgr, a cell division gene of *Drosophila melanogaster*. *J. Cell Sci.* **89**, 39–47.

HARTWELL, L. H. (1978). Cell division from a genetic perspective. *J. Cell Biol.* **77**, 627–637.

HARTWELL, L. H., CULOTTI, J. R. AND REID, B. J. (1974). Genetic control of the cell division cycle in yeast. *Science* **183**, 46–51.

HARTWELL, L. H. AND WEINERT, T. A. (1989). Checkpoints: Controls that ensure the order of cell cycle events. *Science* **246**, 629–633.

INGHAM, P. W. (1988). The molecular genetics of embryonic pattern formation in *Drosophila*. *Nature* **335**, 25–34.

KARR, T. L. AND ALBERTS, B. M. (1986). Organization of the cytoskeleton in early *Drosophila* embryos. *J. Cell Biol.* **102**, 1494–1509.

KELLOGG, D. R., MITCHISON, T. J. AND ALBERTS, B. M. (1988). Behavior of microtubules and actin filaments in living *Drosophila* embryos. *Development* **103**, 675–686.

LEHNER, C. F. AND O'FARRELL, P. H. (1989). Expression and function of *Drosophila* cyclin A during embryonic cell cycle progression. *Cell* **56**, 957–968.

LEWIS, E. B. (1978). A gene complex controlling segmentation in *Drosophila*. *Nature* **276**, 565–570.

LINDSLEY, D. L. AND NOVITSKI, E. (1957). Localization of the genetic factors responsible for the kinetic activity of X chromosomes of *Drosophila melanogaster*. *Genetics* **43**, 790–798.

MCINTOSH, J. R. (1984). Mechanisms of mitosis. *Trends Biochem Sci.* **9**, 195–198.

MILLER, K. G., FIELD, C. M. AND ALBERTS, B. A. (1989). Actin binding proteins from *Drosophila* embryos: a complex network of interacting proteins detected by F-actin affinity chromatography. *J. Cell Biol.* **109**, 2963–2975.

MINDEN, J. S., AGARD, D. A., SEDAT, J. W. AND ALBERTS, B. A. (1989). Direct cell lineage analysis in *Drosophila melanogaster* by time-lapse three dimensional optical microscopy of living embryos. *J. Cell Biol.* **109**, 505–516.

MITCHISON, T. J. AND SEDAT, J. W. (1983). Localisation of antigenic determinants in whole *Drosophila* embryos. *Devl Biol.* **99**, 261–264.

MURRAY, A. W. (1989). The cell cycle. *Am. Zool.* **29**, 511–522.

NEWPORT, J. AND KIRSCHNER, M. (1982). A major developmental transition in early *Xenopus* embryos: I. Characterization and timing of cellular changes at the midblastula stage. *Cell* **30**, 675–686.

NOVITSKI, E. (1955). Genetic measures of centrosome activity in *Drosophila melanogaster*. *J. cell. comp. Physiol.* **45**, 151–168.

PICKETT-HEAPS, J. D., TIPPET, D. H. AND PORTER, K. R. (1982). Rethinking mitosis. *Cell* **29**, 729–744.

RABINOWITZ, M. (1941). Studies on the cytology and early embryology of the egg of *Drosophila melanogaster*. *J. Morph.* **69**, 1–49.

RAFF, J. W. AND GLOVER, D. M. (1988). Nuclear and cytoplasmic mitotic cycles continue in *Drosophila* embryos in which DNA synthesis is inhibited with aphidicolin. *J. Cell Biol.* **107**, 2009–2019.

RAPPAPORT, R. (1971). Cytokinesis in animal cells. *Int. Rev. Cytol.* **31**, 169–213.

SANDLER, L. (1977). Evidence for a set of closely linked autosomal genes that interact with sex-chromosome heterochromatin in *Drosophila melanogaster*. *Genetics* **86**, 567–582.

SCHUPBACH, T. AND WIESCHAUS, E. (1989). Female sterile mutations on the second chromosome of *Drosophila melanogaster* I. Maternal effect mutations. Genetics **121**, 101–117.

SMITH, D. A., BAKER, B. S. AND GATTI, M. (1985). Mutations in genes controlling essential mitotic functions in *Drosophila melanogaster*. *Genetics* **110**, 647–670.

SONNENBLICK, B. P. (1950). The early embryology of *Drosophila melanogaster*. In *Biology of* Drosophila (ed. M. Demerec), pp. 62–167. New York: John Wiley and Sons. Reprinted in 1965, New York and London: Hafner.

STAFSTROM, J. P. AND STAEHELIN, L. A. (1984). Dynamics of the nuclear envelope and nuclear pore complexes during mitosis in the *Drosophila* embryo. *Eur. J. Cell Biol.* **34**, 179–189.

SULLIVAN, W. (1986). Heterochromatic elements which function early in *Drosophila* embryogenesis. Thesis, University of Washington, Seattle.

SULLIVAN, W. (1987). Independence of *fushi tarazu* expression with respect to cellular density in *Drosophila* embryos. *Nature* **327**, 164–167.

SUNKEL, C. E. AND GLOVER, D. M. (1988). *polo*, a mitotic mutant of *Drosophila* displaying abnormal spindle poles. *J. Cell Sci.* **89**, 25–38.

WANG, R. J., WISSINGER, W., KING, E. J. AND WANG, G. (1983). Studies on cell division in mammalian cells. VII A temperature sensitive cell line in abnormal centriole separation and chromosome movement. *J. Cell Biol.* **96**, 301–306.

WARN, R. N., FLEGG, L. AND WARN, L. (1987). An investigation of microtubule organization and functions in living *Drosophila* embryos by injection of a fluorescently labeled antibody against tyrosinated tubulin. *J. Cell Biol* **105**, 1721–1730.

WEINERT, T. A. AND HARTWELL, L. H. (1988). The RAD9 gene controls the cell cycle response to DNA damage in *Saccharomyces cerevisiae*. *Science* **241**, 317–322.

ZALOKAR, M., AUDIT, C. AND ERK, I. (1975). Developmental defects of female sterile mutants of *Drosophila melanogaster*. *Devl Biol.* **47**, 419–432.

ZALOKAR, M. AND ERK, I. (1976). Division and migration of nuclei during early embryogenesis of *Drosophila melanogaster*. *J. microsc. biol. Cell* **25**, 97–106.

ZUSSMAN, S. B. AND WIESCHAUS, E. (1987). A cell marker system and mosaic patterns during early embryonic development in *Drosophila melanogaster*. *Genetics* **115**, 725–736.

(*Accepted 11 July 1990*)